Holographic Composites with Gold Nanoparticles: Nanoparticles Promote Polymer Segregation

Leonid M. Goldenberg,*[,†,#] Oksana V. Sakhno,[†,#] Tatiana N. Smirnova,[‡] Phil Helliwell,[§] Victor Chechik,[§] and Joachim Stumpe[⊥]

UP Transfer GmbH at the University of Potsdam, Am Neuen Palais 10, 14469 Potsdam, Germany, Institute of Physics, National Academy of Science, Kiev, Ukraine, Department of Chemistry, University of York, Heslington, York YO10 5DD, U.K., and Fraunhofer Institute for Applied Polymer Research, Science Campus Golm, Geiselbergstr. 69, 14476 Potsdam, Germany

Received February 22, 2008. Revised Manuscript Received May 19, 2008

New nanocomposites containing functionalized acrylate monomers and Au nanoparticles (NPs, 1.5−3 nm core diameter, 1−2 wt %) have been developed for an all-optical fabrication of periodic bulk structures by holographic photopolymerization. The Au NPs were coated with ethyl 11-mercaptoundecanoate to ensure good solubility in low-polarity organic media. The materials with only 1.5 wt % Au NPs show unusually high amplitude of the refractive index modulation in the diffraction volume gratings (0.0073). Both volume and surface relief gratings are formed during the holographic exposure. The proposed mechanism of the refractive index contrast amplification (as compared to monomer mixture without NPs) includes interception of free radicals by Au nanoparticles. This slows down the free-radical photopolymerization, thus promoting the increase in lateral periodic redistribution of the components in the interference pattern. The redistribution of both NP and monomers provides high efficient grating formation with the spatial period of 0.5−4.5 μm. The formation of the surface relief coincident with the interference pattern is also observed. The introduction of 1.5 wt % Au NPs into the prepolymer mixture more than doubles the surface relief depth (from ca. 150 to 400 nm for the period 4.2 μm), thus proving the NP influence on the structure and, consequently, on the shrinkage of the polymer matrix.

1. Introduction

Polymer composites containing metal nanoparticles (NP) have attracted immense attention due to their potential applications, for example, in catalysis, bioengineering, photonics, and electronics.[1a] Metal NP exhibit unique optical properties in the visible spectral range due to the collective excitation of conducting electrons known as surface plasmons.[1b,c] The local field enhancement contributes to the enhancement of linear and nonlinear optical transitions, which gives rise to the enhancement of fluorescence,[2a] Raman scattering,[2b] two-photon excitation,[2c] and modification of the radiative decay properties of the fluorescent molecules.[2d] All these properties can be utilized in a number of applications such as apertureless near-field microscopy and spectroscopy, surface-enhanced Raman spectroscopy, and radiative decay engineering.

The use of periodically ordered metal microstructures (gratings) opens up new practical possibilities by providing the coupling between the light wave and surface plasmons. This allows conversion of the light wave into the plasmon wave that can serve as a powerful basis for designing new optical diffractive elements with ultrahigh spectral dispersion.[3a] Periodic structures serving as resonators for lasing also attract significant attention. The use of the distributed feedback resonators based on two-dimensional Au-disk photonic crystal template[1d] and Au-NP-polymer gratings[3b] ensure the low-threshold lasing in thin-film waveguide structures.

Periodic distribution of the additional neutral component within the bulk of polymer film during holographic exposure is explained by the photopolymerization-induced counterdiffusion of the components due to imbalance of the concentration of the mixture components in the regions of the film corresponding to the bright and dark regions of the interference pattern. Bunning and co-workers[4a] pioneered the use of NP (polymer, clay, and metal) with substantially higher (or lower) refractive index (n), as a movable nonreactive component in holographic photocurable organic mixtures. The idea has been further developed using different metal oxide NP[4b–e] (TiO_2, ZrO_2). This increased the amplitude of the refractive index modulation n_1 (the difference between refractive indices of the neighboring grating planes divided by two) up to 0.024.[4f] Photoluminescent lanthanide NP were used to develop volume transmission holograms performing a light emission in the grating planes enriched by the NP, which can be used for optical security applications.[4g]

* Corresponding author. Tel.: +49 331 568 1261. Fax: +49 331 568 3259. E-mail: lengold@gmx.de.
† UP Transfer GmbH.
‡ National Academy of Science.
§ University of York.
⊥ Fraunhofer Institute for Applied Polymer Research.
Present address: Institute of Thin Film Technology and Microsensorics, c/o Fraunhofer Institute for Applied Polymer Research, Science Campus Golm, Geiselbergstr. 69, 14476 Potsdam, Germany.

10.1021/cm8005315 CCC: $40.75 © 2008 American Chemical Society
Published on Web 06/25/2008

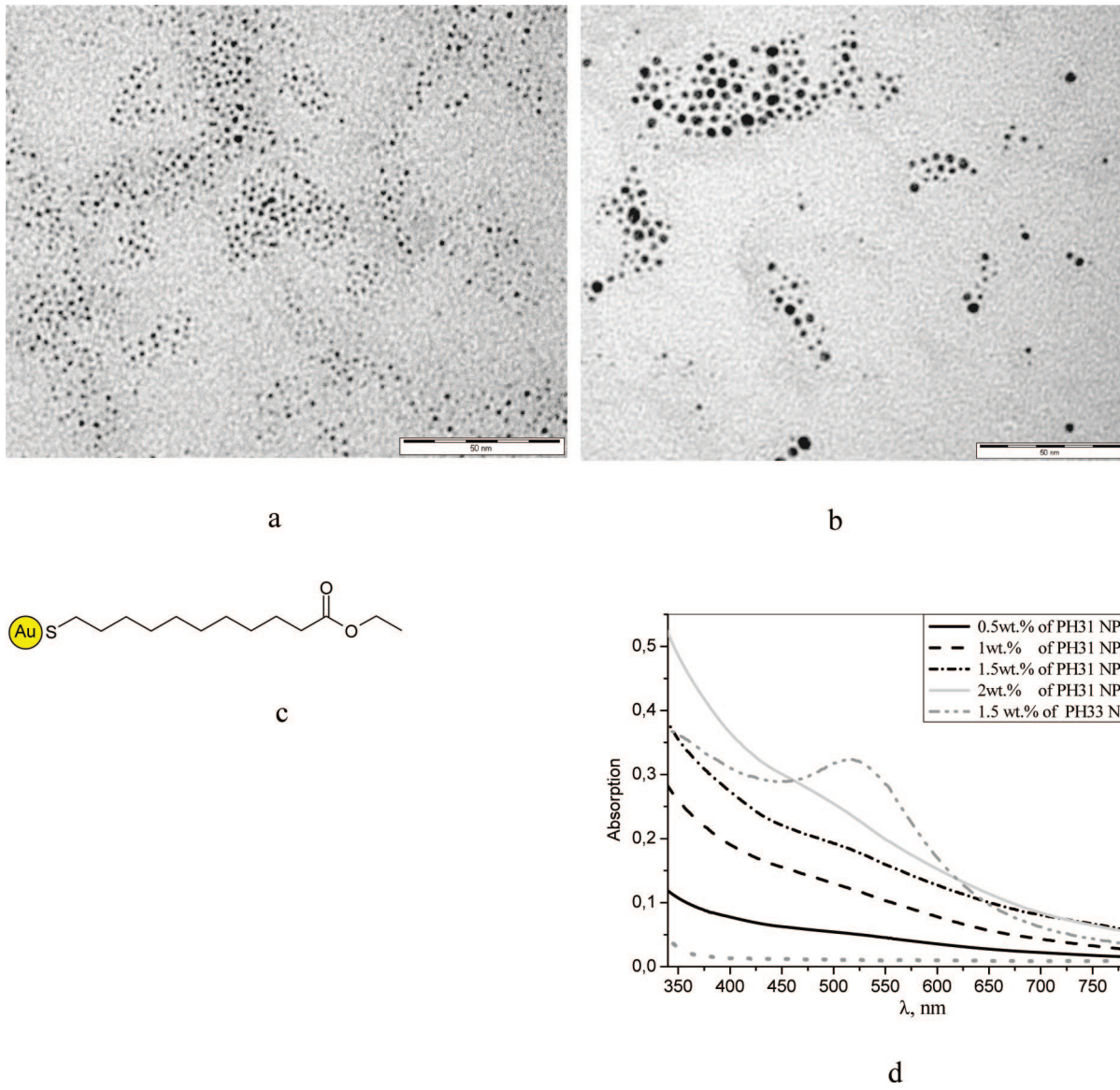

Figure 1. (a,b) TEM images of PH31 and PH33 Au NP, respectively. (c) Schematic representation of the Au NP protected by ester-terminated alkanethiol. (d) Absorption of the solid films prepared from the composite with different amounts of Au NP.

Au NP were first applied to holographic photopolymers by Bunning and co-workers.[4a] However, only weak diffraction efficiency (η) of about 0.3 (20 μm grating thickness, with 5 nm Au NP in ca. 5 wt %) was achieved in these experiments. Further development of the curable photopolymer composite containing metal NP suitable for holographic structuring has not been attempted.

Here, we report on the new effective holographic metal NP-containing monomer composites. They consist of the photopolymerizable acrylate blend and low loading of Au NP (0.5−2 wt %). We have shown that high η of the volume gratings (up to 0.6) cannot be explained by the spatial redistribution of the NP in photocurable organic material (usual mechanism in similar materials).[4a–g] The high efficiency of NP-containing composites was tentatively explained by the retardation of free radical polymerization by the Au NP, which leads to a change in the kinetics of photopolymerization and diffusion of the components that consequently causes much higher periodical segregation of the monomers between the grating planes.

2. Experimental Section

2.1. Materials. Ethyl 11-mercaptoundecanoate (Figure 1c) was prepared following a literature procedure.[5a] This ligand was used to coat Au nanoparticles. The long alkane chain in the ligand provided for high stability in solution and holographic mixture while the ester functionality ensured good solubility properties. The small Au nanoparticles (PH31) were prepared following a modified method of Brust et al.[5b] A 1% aqueous $HAuCl_4$ (5 mL) was mixed with a solution of tetraoctylammonium bromide (350 mg) in toluene (15 mL) and stirred for 10 min. To this mixture, ethyl 11-mercaptoundecanoate (30 mg) was added and the stirring continued for 5 min. A solution of $NaBH_4$ (50 mg) in water (5 mL) was then added to the vigorously stirred reaction mixture. The reaction was quenched after 30 s by addition of 0.5 M HCl (20 mL) to prevent base-catalyzed hydrolysis of the ester group. The organic phase was separated and washed with saturated aqueous $NaHCO_3$ (20 mL) and water (20 mL). The solvent was removed by evaporation; the crude NP were dissolved in dichloromethane and purified using gel permeation chromatography with BioBeads SX-1 gel (Bio-Rad). The nanoparticles were characterized by ^{1}H NMR, UV spectroscopies, TGA, and TEM. ^{1}H NMR, $CDCl_3$, δ, ppm: 4.1 br s

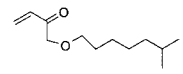

IOA, n=1.434, ρ=0.88 g/mL, M=184

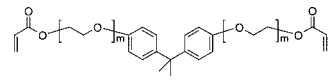

EBPDA, EO/phenol 1.5, n=1.545, ρ=1.146 g/mL, M=468

Figure 2. Acrylate monomers used as a photocurable part of the nanocomposites.

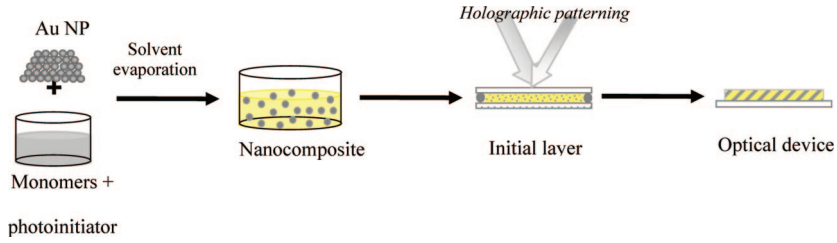

Figure 3. Schematic of the nanocomposite preparation and optical diffractive element fabrication.

(3H, CH_3O), 2.2 br s (2H, CH_2CO), 0.9−1.7 (16H, CH_2). TGA measurement showed 69 wt % metal in the NP (at 250−310 °C). UV spectra show a weak shoulder at 520 nm. TEM investigation of the NP (PH31) (Figure 1a) synthesized shows that the NP are mostly spherical and the average Au core diameter was evaluated as 1.7 ± 0.3 nm.

For evaluation of the influence of particle size on the holographic properties of the composites, the NP with a larger core size (PH33) were prepared by reducing Au(III) in the presence of tetraoctylammonium bromide.[5c] To coat the NP with the same protection ligand, the ligand exchange reaction of ethyl 11-mercaptoundecanoate with tetraoctylammonim-stabilized Au NP was carried out. One percent aqueous $HAuCl_4$ (2.5 mL) was mixed with a solution of tetraoctylammonium bromide (175 mg) in toluene (7.5 mL) and stirred for 15 min. To this mixture, a solution of $NaBH_4$ (25 mg) in water (2.5 mL) was then added with vigorous stirring. The reaction was quenched after 30 s by addition of 0.5 M HCl (10 mL). The organic phase was separated and washed with saturated aqueous $NaHCO_3$ (10 mL) and water (10 mL). The organic phase was then reduced to ca. 4 mL using a rotary evaporator and mixed with a 10^{-2} M solution of ethyl 11-mercaptoundecanoate in toluene (800 μL). The reaction mixture was left for 20 h, the solvent was removed by evaporation, and the NP were dissolved in dichloromethane and purified using gel permeation chromatography with BioBeads SX-1 gel (Bio-Rad). NMR spectra were identical to those of the smaller NP. The average Au core diameter of these NP has been determined from TEM images as 2.7 ± 0.8 nm (Figure 1b, PH33). TGA investigation of NP showed the loss of ca. 18% mass at 250−310 °C.

Holographic syrups we employed in this investigation are homogeneous mixtures of commercially available mono- and multifunctional acrylate monomers. The selection of the photocurable components for holographic nano-photopolymers is crucial. It has to be a good dispersive media for the NP, has to allow the redistribution of the NP within a curing organic media during the holographic patterning without aggregation, and provide for a high stability of the final structure. The choice of the organic components was governed by the previous investigation.[4c,e–g] It was shown that the best results are obtained by using the mixtures of single- and multifunctional acrylate monomers, which polymerize independently with substantially different rates. The chemical formulas of the monomers used, their refractive indices, density, and average molecular weight are shown in Figure 2.

Isooctylacrylate (IOA) is a low-viscosity, nonpolar, low-shrinkage monofunctional monomer, and ethoxylated bisphenol A diacrylate (EBPDA) is a bifunctional low-shrinkage monomer, which generates an insoluble cross-linked network. Other monomer combinations[4g] exhibited much lower grating efficiency. The monomers (Aldrich) were used as-received. Free-radical photoinitiator Irgacure 1700 (Ciba-Geigy) (1.5 wt %) was added to the syrup to provide the sensitivity to UV light (365 nm).

The concentrations of IOA and EBPDA in the prepolymer syrup were optimized according to their holographic performances. The highest recording efficiency and shortest time of the light exposure were obtained for the ratio IOA:EBPDA = 80:20 wt %. The Au NP were first dispersed in CH_2Cl_2, followed by the mixing with the prepolymer syrup containing the photoinitiator (Figure 3). After natural evaporation of the solvent the final composites with different Au NP content (0−2 wt %) were used for the investigations. The composites containing PH31 and PH33 NP were stable for at least 2 weeks.

2.2. Measurements. The absorption spectra were registered using a Perkin-Elmer Lambda 2 spectrometer for films and reflection microscope-spectrometer TIDAS/MSP system from J@M (lateral resolution ca. 2 μm, maximum amplification 70) for gratings with a 4.2 μm period. The thickness of the films (accuracy of about 0.2 μm) was measured by a Dectack profilometer after disassembly of the cell. An Abbe refractometer was used to determine the refractive index of the monomers and the nanocomposites. Optical microscopic images of the grating were obtained by a Zeiss Axioplan 2 microscope. The surface topology of the gratings was examined by atomic force microscopy performed using a Solver P47H Smena instrument (NTMDT, Russia) in semicontact mode after disassembly of the cell.

Photopolymerization kinetics of the nanocomposites sandwiched between two CaF_2 slides (cell thickness ca. 200 μm) was tested by FTIR spectroscopy (Mattson Instruments RS 10000 FTIR). Flood exposure during FTIR measurements and that of gratings after holographic writing was performed using a Philips PL 10W-10 UV lamp with the average intensity 2 mW/cm^2 (average emission wavelength is 365 nm). The constant value of the curing intensity was maintained by ensuring the equal distance between the lamp and the sample.

A drop of the initially liquid nanocomposite was placed between two glass slides separated by the spacers of a proper thickness (ca. 20 μm). For recording of the grating a typical setup of transmission geometry based on an Ar ion laser emitting at $\lambda_r = 364$ nm (s-polarization) described earlier was used. A low-intensity He−Ne laser beam ($\lambda_t = 633$ nm, s-polarization) placed at the Bragg angle, corresponding to the proper spatial period of the grating, was used for real-time monitoring of the grating formation. η of the gratings was calculated as $\eta = I_{dif}/(I_{tr} + I_{dif})$ where I_{tr} and I_{dif} are the

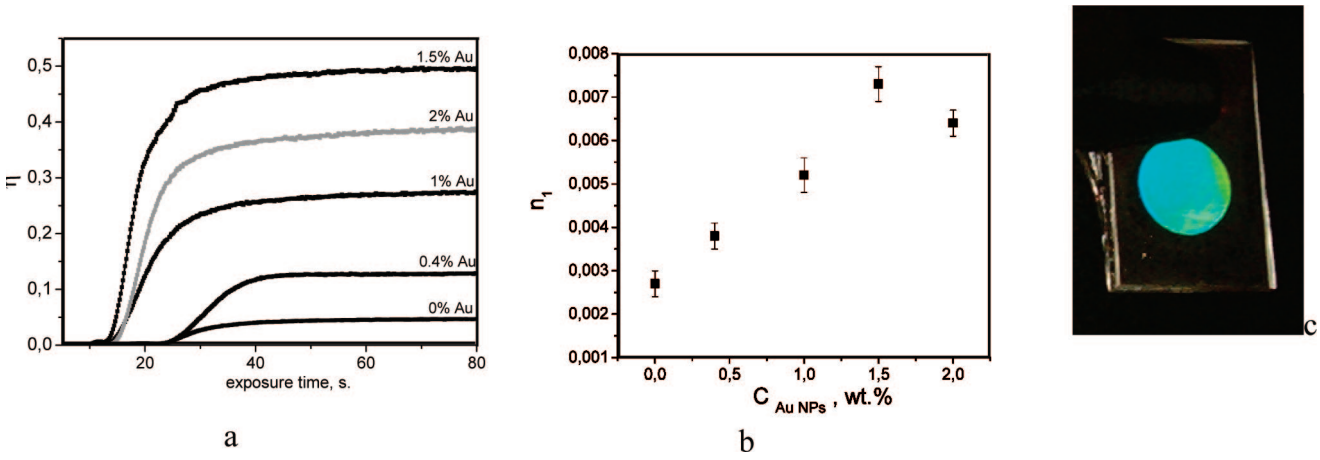

Figure 4. (a) Grating recording kinetics ($\eta(t_{exp})$) for the composite containing different concentrations of PH31 NP. (b) Refractive index modulation amplitude (n_1) as a function of the NP concentration (C_{NP}). Grating period is $\Lambda = 0.98$ μm; writing intensity is ca. 6 mW/cm^2. (c) Photo of the grating illuminated with white light.

intensities of the transmitted and the diffracted (−1st order) beams, respectively. This way, reflected, scattered light, and a linear absorption were excluded from the calculation of η. Samples were typically exposed for 80−150 s with the intensity 3−10 mW/cm^2. The period of the grating (Λ) was varied in the range 0.5−4.4 μm by changing the angle between the recording beams (2Ω), $\Lambda = \lambda_r/2 \sin \Omega$.

The gratings with spatial period 0.5−1.5 μm and thickness of ca. 20 μm were Bragg (volume) gratings according to Cook-Klein parameter;[6] only 0 and −1 diffraction order were observed in the diffraction pattern. The experimentally measured angular dependence of η of the gratings containing 1−1.5 wt % Au NP (λ_t = 633 nm, s-polarization) showed good fit with the Kogelnik's formula for η of phase thick grating.[7] Good agreement with the theory made it possible to use the Kogelnik's formula for further calculation of n_1:

$$n_1 = \frac{\lambda_t \cos \theta_B \arcsin \sqrt{\eta}}{\pi d} \quad (1)$$

where θ_B is the Bragg angle within the material. In the diffraction pattern of the gratings with spatial period >2 μm several higher diffraction orders were also observed that confirmed the Raman-Nath diffraction regime.

For TEM measurements a piece of the grating was placed in LR White resin for 2 h at room temperature on a rotator. It was put in a gelatin capsule, which was filled with resin and sealed and left at 40 °C over the weekend. Sections were cut at around 90 nm on a Leica Ultracut microtome, collected on a 200 mesh copper grid with a Formvar/carbon support film, and imaged using FEI Tecnai 12 TEM at 120 kV.

3. Results

3.1. Holographic Recording of Volume Gratings. Temporal evolution of the grating ($\eta(t_{exp})$) in the composites with different NP (PH31) content and the maximum values of n_1 achieved as a function of the NP concentration (C_{NP}) are presented in Figures 4a and 4b, respectively. A typical image of the white light-illuminated grating is shown in Figure 4c. In the basic prepolymer syrup without NP, the formation of a stable grating with maximum η of only 0.08 ($n_1 \approx 0.0027$) was observed. The introduction of even a small amount of Au NP (1 wt %) causes a significant growth of the grating η to ca. 0.3. The maximum values of n_1 of ca. 0.0073 were obtained for the NP concentration in the range of 1.4−1.6 wt %. Further increase in C_{NP} to 2 wt % leads to the decrease in final $\eta \approx 0.4$. The writing intensity also affects the recording rate and the efficiency of the gratings both in the pure monomer mixture (Figure 5a) and in the mixture with Au NP (Figure 5b). The $n_1(I)$ dependence for the composite with 1.5 wt % Au NP (Figure 5b) shows that n_1 (and the recording rate) reaches its maximum value in a narrow intensity range (6−9 mW/cm^2). Such a dependence $n_1(I)$ is typical for photopolymers and it will be discussed below.

(1) (a) Bronstein, L. M.; Valetsky, P. M.; Antonietti, M. In *Nanoparticles and nanostructures films. Preparation, characterisation and applications*; Fendler, J., Ed.; Wiley-VCH: Weinheim, 1998. (b) Kreibig, U.; Vollmer, M. *Optical properties of metal clusters; Springer series in material science*; Springer: Berlin, 1995. (c) Kelly, K. L.; Coronado, E.; Zhao, L. L.; Schatz, G. C. *J. Phys. Chem. B* **2003**, *107*, 668. (d) Stehr, J.; Grewett, J.; Shimdler, F.; Sperling, R.; von Plessen, G.; Lemmer, U.; Lupton, J. M.; Klar, T. A.; Feldman, J.; Holleitner, A. W.; Forster, M.; Scherf, U. *Adv. Mater.* **2003**, *15*, 1726.

(2) (a) Sokolov, K.; Chumanov, G.; Cotton, T. M. *Anal. Chem.* **1998**, *70*, 3898. (b) Chang, R. K., Furtak, T. A., Eds.; *Surface-enhanced Raman-scattering*; Plenum: New York, 1982. (c) Shalaev, V. M. In Nonlinear Optics of Random Media: Fractal Composites and Metal Dielectric Films. *Springer Tracts in Modern Physics*; Springer: Berlin, 2000. (d) Lakowicz, J. R. *Anal. Biochem.* **2001**, *298*, 1.

(3) (a) Mikhailov, V.; Elliott, J.; Wurtz, G.; Bayvel, P.; Zayats, A. V. *Phys. Rev. Lett.* **2007**, *99*, 083901. (b) Fukushima, M.; Yanagi, H.; Hayashi, S.; Sugamura, N.; Taniguchi, Y. *J. Appl. Phys.* **2005**, *97*, 106104.

(4) (a) Vaia, R. A.; Dennis, C. L.; Natarajian, L. V.; Tondiglia, V. P.; Tomlin, D. W.; Bunning, T. J. *Adv. Mater.* **2001**, *13*, 1570. (b) Suzuki, N.; Tomita, Y.; Kojima, T. *Appl. Phys. Lett.* **2002**, *81*, 4121. (c) Smirnova, T. N.; Sakhno, O. V.; Bezrodnyi, V. I.; Stumpe, J. *Appl. Phys. B: Laser Opt.* **2005**, *80*, 947. (d) Sanchez, C.; Escuti, M. J.; van Heesch, C.; Bastiaansen, C. W. M.; Broer, D. J.; Loos, J.; Nussbaumer, R. *Adv. Funct. Mater.* **2005**, *15*, 1623. (e) Sakhno, O. V.; Goldenberg, L. M.; Stumpe, J.; Smirnova, T. N. *Nanotechnology* **2007**, *18*, 105704. (f) Garnweitner, G.; Goldenberg, L. M.; Sakhno, O. V.; Antonietti, M.; Niederberger, M.; Stumpe, J. *Small* **2007**, *3*, 1626. (g) Sakhno, O. V.; Smirnova, T. N.; Goldenberg, L. M.; Stumpe, J. *Mater. Sci. Eng., C* **2008**, *28*, 28.

(5) (a) Koenig, N. H.; Sasin, G. S.; Swern, D. *J. Org. Chem.* **1958**, *23*, 1525. (b) Brust, M.; Walker, M.; Bethell, D.; Schiffrin, D. J.; Whyman, R. *Chem. Commun.* **1994**, 801. (c) Fink, J.; Kiely, C. J.; Bethell, D.; Schiffrin, D. J. *Chem. Mater.* **1998**, *10*, 922.

(6) Colier, R. J.; Burckhardt, C. B.; Lin. L. Y. *Optical holography 1971*; Academic Press: New York, 1973; 686 pp.

(7) Kogelnik, H. *Bell Syst. Tech. J.* **1969**, *48*, 2909.

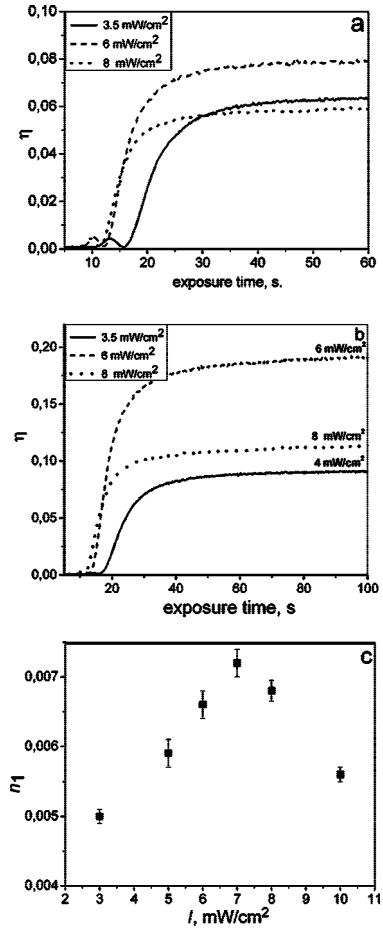

Figure 5. (a) Intensity dependence of η of the grating without Au NP. (b) Intensity dependence of η of the grating with 1 wt % Au NP. (c) n_1 as a function of the recording intensity for the optimized composite content with 1.5 wt % Au NP. Grating period is 0.98 μm.

The above holographic results were obtained for the nanocomposite containing PH31 NP with the average core size of ca. 1.7 nm. The composites containing 1.5 wt % of PH33 with the average core size of 2.7 nm perform similarly. The maximum achieved n_1 was about 0.0075 for 1.5 wt % NP. Thus, we did not observe the influence of the NP size on the holographic properties, probably due to the insufficient size range of the NP studied.

3.2. Influence of the Au NP on the Monomer Photopolymerization. The kinetics of the photocuring of the composites without and with Au NP (PH31) under homogeneous UV illumination has been studied. The monomer conversion was evaluated by monitoring the intensity of the C═C peak in the acrylates (ca. 1640 cm^{-1}) and using the formula $C(t) = (A_0 - A(t))/A_0$, where A_0 and $A(t)$ correspond to absorption of the film before and during the UV exposure (Figure 6). The rate of photopolymerization for the pure monomer syrup and the composites with Au NP are shown in the insert of Figure 6. The rate of polymerization is the highest for the pure monomer mixture and decreases with the increased Au NP content in the composite. The induction period of photopolymerization (defined as the time required for consumption of dissolved oxygen) is the shortest for pure monomer composite and also increases with the increase in C_{NP}. The conversion of all composites does not exceed 0.6.

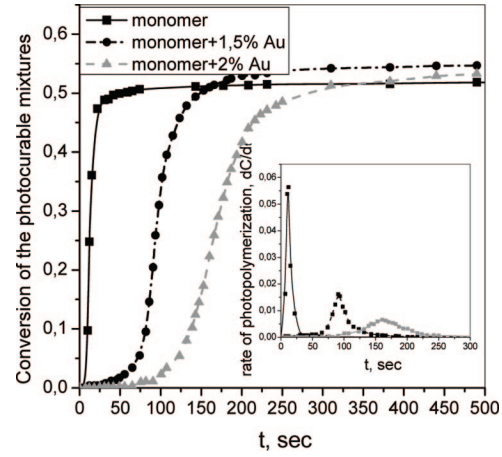

Figure 6. Monomer conversion from FTIR data in the composite without and with 1.5 and 2 wt % of Au NP (PH31). The insert shows the polymerization rate of mentioned materials.

Table 1. Surface Relief Height of the Grating with Different Grating Period, Recorded in Pure Monomer Blend and the Composites Containing 1.5 wt % of Au NP

composite	EBPDA20:IOA80 0 wt % Au NP	EBPDA20:IOA80 1.5 wt % Au NP
$h(\Lambda = 0.9\ \mu m)$, nm	20 ± 5	50 ± 10
$h(\Lambda = 2.25\ \mu m)$, nm	90 ± 10	190 ± 10
$h(\Lambda = 4.2\ \mu m)$, nm	130 ± 20	390 ± 20

3.3. Surface Topology of the Gratings. The surface topology of the gratings recoded in the nanocomposites was also investigated. The surface relief amplitude depends on the material formulation and spatial period of the structure (Table 1). Notable is the significant increase in depth in the whole range of the grating periods for the optimal nanocomposite content (1.5 wt % Au NP) compared to those in a pure monomer mixture. The relief height of the grating changes from 25 to 130 nm for a pure monomer mixture and from 50 to almost 400 nm (depending on the grating period) for the optimal nanocomposite content. The increase in the surface relief with the period is typical for photopolymerizable holographic materials and will be discussed below. 3D surface topology and cross section of the grating with the period 4.2 μm is shown in Figure 7.

4. Discussion

4.1. Volume Material Modulation. In contrast to the photocurable composites containing metal oxide NP,[4b–g] where grating formation is mainly determined by the mass transfer of the NP within the polymer matrix, in the Au NP containing composites C_{NP} is so small that their spatial distribution between the grating planes cannot provide appreciable refractive index contrast. Using a simple reaction/diffusion model for the grating formation in the mixtures comprising two reactive monomers only and the monomers with nonreactive NP (Figure 8), we have estimated the influence of the component distribution on the value of n_1.

In the initial state, the composite is an equilibrium mixture of the components (Figure 8). The polymerization in the maxima of the interference pattern disturbs the thermodynamic equilibrium of the system, creating the gradient in the chemical potential of each component that in turn causes

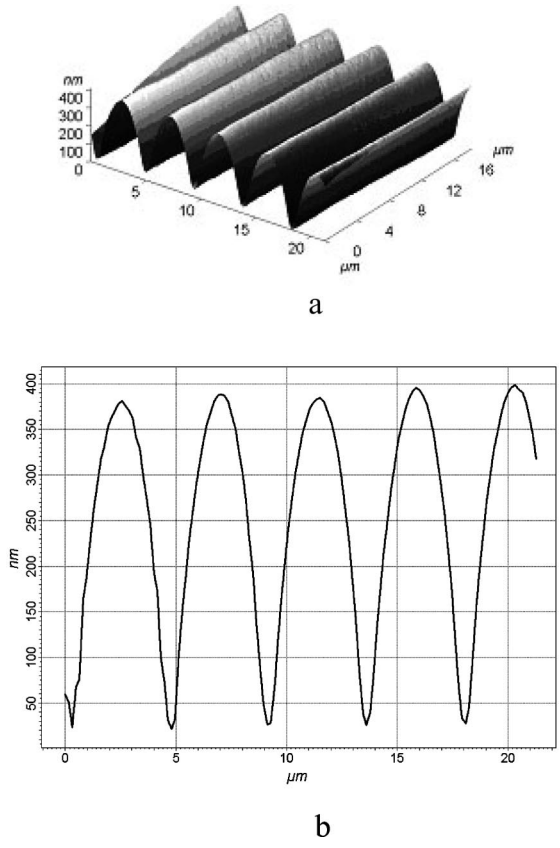

Figure 7. Surface topology and cross section of the gratings in the material with 1.5 wt % Au NP, $\Lambda = 4.2$ μm.

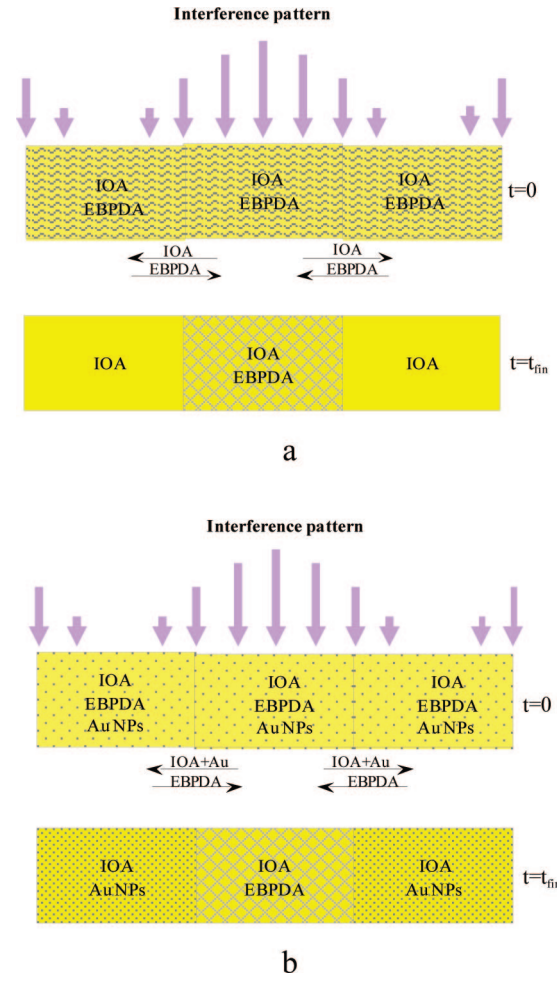

Figure 8. Schematic representation of the volume grating formation in a pure monomer mixture (a) and in the composite with Au NP (b).

their diffusive redistribution between the low- and high-intensity areas. This results in a spatial modulation of the chemical composition and average refractive index of the material forming the image of the interference pattern.

The model assumes that the redistribution of the components occurs at a constant volume of the system; the polymer shrinkage is neglected. Two cases of the component redistribution, which result in the highest possible modulation of the average refractive index, are shown in Figure 8. For the two-monomer composite (Figure 8a), the polymer network originated from the multifunctional EBPDA with equilibrium content of IOA will be formed in the high-intensity areas. The polymer enriched by IOA fraction will be localized in the low-intensity areas. In the three-component mixture, containing Au NP (Figure 8b), there is a contribution from the NP segregation as well.

Using the approximate formulas determining the refractive index modulation in two- and three-component mixtures[8,4g] and the corresponding volume fraction of the components, we calculated maximum possible n_1 as 0.0157 for the system in Figure 8a (n for pure polymers were measured by an Abbe refractometer as 1.573 and 1.475 for EBPDA and IOA, respectively).

However, the maximum experimental value of n_1 was only 0.0027, which confirms that the real segregation of the monomers is far from complete. Similarly, for the composite with 1.5 wt % Au NP at the second boundary case (shown in Figure 8b), the evaluated value of n_1 was 0.0167. The following values for the real part of the refractive index of Au in the spectral range 500−650 nm and density $n_{NP} = 0.2$ and $\rho = 20$ g/mL[9] were used for the calculations. It means that a possible contribution of the NP into n_1 is only 0.001, which is insignificant compared to the experimental value of 0.0073.

Besides, with use of the mentioned formula,[8,4g] the modulation of the monomer (IOA) concentration Δv_M (Δv_M is the difference between the volume fraction of the monomer in the bright and the dark regions) can be evaluated. In the case in Figure 8a, the maximal achievable value of Δv_M is ca. 0.32. For the grating recorded in the pure monomer mixture this value was calculated as ≅0.055. For the grating containing 1.5 wt % of Au NP, the Δv_M calculated from experimental value of η is ca. 0.122, which is more than double the value of Δv_M for the monomer composite.

The comparison of the experimental value of n_1 with those obtained for the different models leads to the conclusion that the enhancement of the grating efficiency in the composite

(8) Sakhno, O. V.; Smirnova, T. N. *Opt. Spectrosc.* **1998**, *85*, 950.

(9) Caseri, W. *Macromol. Rapid Commun.* **2000**, *21*, 705.

(10) (a) Zhao, G.; Mouroulis, P. J. *J. Mod. Opt.* **1994**, *41*, 1929. (b) Colvin, V. L.; Larson, R. G.; Harris, A. L.; Schilling, M. L. *J. Appl. Phys.* **1997**, *81*, 5913. (c) Karpov, G. M.; Obukhovskii, V. V.; Smirnova, T. N.; Sarbaev, T. A. *Opt. Spectrosc.* **1997**, *82*, 131. (d) Karpov, G. M.; Obukhovsky, V. V.; Smirnova, T. N.; Lemeshko, V. V. *Opt. Commun.* **2000**, *174*, 391.

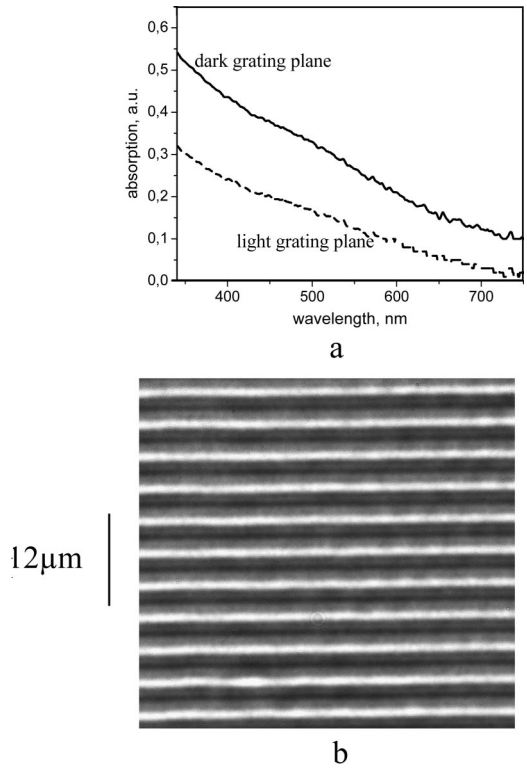

Figure 9. (a) Absorption spectra of the dark and bright fringes of the grating containing 1.5 wt % of Au NP (PH31), $\Lambda = 4.2$ μm, $d = 20$ μm). (b) Optical microscopic image of the grating with 1.5 wt % of Au NP (×100).

containing Au NP is governed not only by the mass transfer of the NP but also mostly by the increase in the segregation of the polymer-forming phases. Thus, in the studied nanocomposites the Au NP are the reactive component, which specifically affects the molecular structure and density of the polymer network that causes the increase in the redistribution of the monomers between the grating planes.

The segregation of the NP was proved by the direct measurement of the absorbance of the material in the adjacent areas of the grating by UV microscopy (Figure 9). The ratio A_{min}/A_{max} for the wavelength 630 nm is approximately equal to 0.5 (Figure 9). It should be noted that the surface relief can also contribute to the absorption change in the grating planes. However, it is easy to show that the variation of A due to the thickness variation is determined by the ratio $A_{min}/A_{max} = 1 - h/d$, where h is the depth of the surface relief. At the grating thickness $d = 20$ μm and $h = 0.4$ μm (see Table 1) the ratio A_{min}/A_{max} is only ca. 0.98. The redistribution of NP was also confirmed by TEM measurements of the grating cross section (Figure 10). The area containing the segregated PH33 NP is shown in Figure 10a, where individual NP are clearly imaged. In Figure 10b, a crossover between the NP reach and the NP-free areas in the adjacent grating planes (light and dark areas of the interference pattern, respectively) is presented.

Since the absorption of the polymer in the spectral range studied here is negligibly small (Figure 1d), the variation in A confirms the redistribution of the Au NP between the grating planes. Notably, the relief modulation substantially decreases with the decreased period. This means that the assumption on the constant total volume of the system during the mass transfer in the evaluation of n_1 can be used to a good approximation.

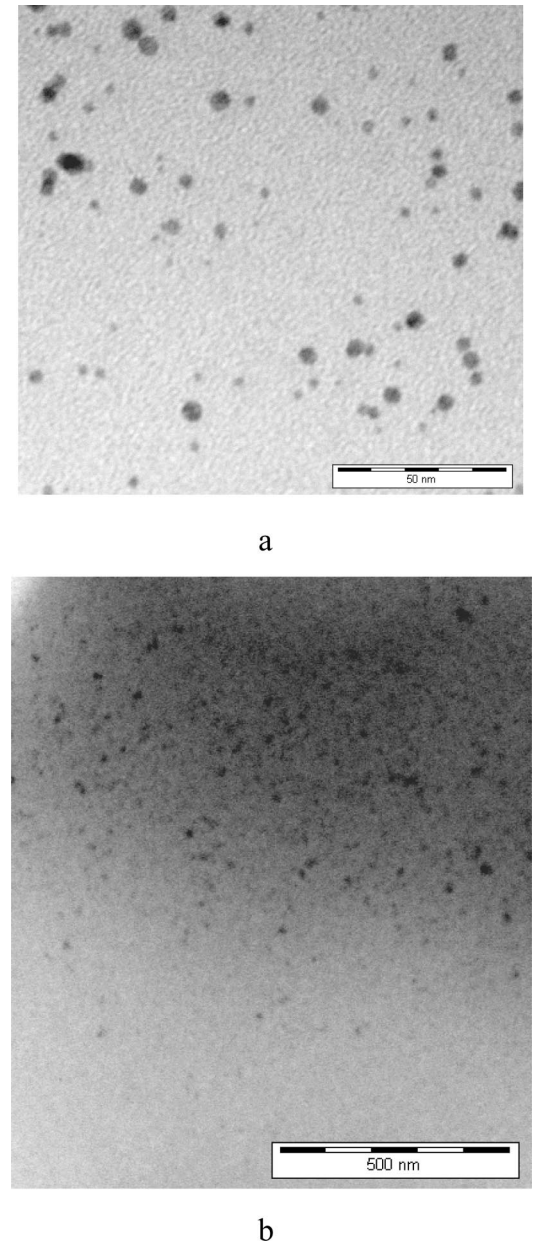

Figure 10. TEM images of PH33 Au NP in holographic volume grating (cross section is approximately perpendicular to the grating planes): (a) the area with a higher C_{NP} at a higher resolution; (b) crossover between the grating planes exhibiting the area with Au NP (upper part) and without Au NP (lower part).

4.2. Kinetics of the Volume Structure Formation. The theory of the grating formation in photopolymerizable materials[10a–d] shows that n_1 and the linearity of the material response are determined by the parameter

$$D_{ef} = (D_0/\Lambda^2)(u_p/I_0'^{1/2}) \quad (2)$$

where u_p is the characteristic rate of polymerization determined by the kinetic parameters of the mixture, D_0 is the diffusion coefficient, $I'_0 = I_0 + I_t$ is the effective average intensity (I_0 is the intensity of the interference pattern; I_t characterizes the decrease in the effective pattern contrast due to polymerization in the dark regions of the interference

pattern caused by scattered light and thermoinitiation by the impurities).

Thus, the value of D_{ef} is determined by the ratio of the characteristic time of polymerization and mass transfer of the components across distance Λ and, consequently, reflects the interdependence between these processes. At $D_{ef} \ll 1$, when the diffusion rate is much smaller than the polymerization rate, the composite can be considered as a single-component material that does not give a stable grating. On the other hand, at $D_{ef} \ll 1$ the diffusion mass transport is so fast that at each moment of time the system remains in a thermodynamic equilibrium state (from the point of view of the diffusion mass transfer). This gives a maximum value of n_1. D_{ef} can also be used to explain the influence of the recording intensity on the holographic performance. For $D_{ef} > 1$, there is a range of the intensities $I_0/I_t \gg 1$, at which n_1 is maximum and does not depend on I.

The time evolution of the gratings recorded in the composite without and with Au NP (Figures 4, 5) shows that the rate of the mass transport of the components exceeds the rate of polymerization, which ensures a smooth growth of η to a steady-state value. A small initial peak on the recording kinetics for the composite without NP corresponds to the formation of two subgratings (polymerization and diffusion) that we discussed earlier.[4g] Relatively high diffraction efficiency of grating recorded in a pure monomer mixture EBPDA:IOA ($\eta \approx 0.08$) resulted from a high difference between the refractive indices of the polymers ($n_{EBPDA} - n_{IOA} = 0.108$).

According to the determination of D_{ef}, the decreasing polymerization rate, observed with the introduction of the Au NP to the monomer blend, can increase the recording efficiency.

Using only the variation of the recording intensity and, consequently, the rate of polymerization of the initial mixture, we could not increase n_1 to the value obtained in the composite with an optimal concentration of the Au NP. This confirms the specific influence of the Au NP on the formation of the polymer network. The catalysis of radical reactions by colloidal metals is well-known.[11] Since the polymerization of the acrylate monomers goes through the free radical mechanism, the introduction of the Au NP can influence the polymerization kinetics and, consequently, change the molecular structure of the final polymer network. The modulation of the polymerization rate by Au NP used in this work can be explained as follows. It is likely that some thiolate groups adsorbed on the Au surface can capture the initiator radicals or participate in the chain transfer during polymerization. This could slow down the initiation step and reduce the molecular weight of polymers formed at the initial stages of the reaction. It is also possible that some active sites on the Au NP can terminate the free radicals via the electron-transfer reactions. The decrease in n_1 with the increased $C_{NP} > 1.5$ wt % could be attributed to the decrease in contrast of the interference pattern, which in turn is caused by the decrease in the polymerization rate.[10c,4g] However, the decrease in n_1 is more likely caused by the specific influence of the NP on the molecular structure of polymer matrix since an insignificant change of C_{NP} leads to an appreciable change of the polymers segregation and increase in the grating diffraction efficiency. More detailed explanation of the influence of the NP on the chemical structure of the polymers constituting the grating planes needs additional investigations.

4.3. Surface Relief in Au NP Contained Composite. Recently, a one-step solvent-free technique for periodic relief structure fabrication based on photopolymerization process has been developed.[12] Theoretical models of this effect were also suggested.[13] It was established that both volume and surface relief modulations result from polymerization-induced mass transfer of the composite components. At that, the shrinkage of the material plays a dominate role in the surface relief formation. Local shrinkage of the medium in the bright areas causes the appearance of extra free volume due to a network formation, so the liquid components can move from the dark into the bright areas. Under these conditions, the volume of the composite in the dark areas decreases in comparison with an initial equilibrium value that causes a spatial modulation of the medium volume which, in turn, is cophased with a spatial intensity distribution. As a result, the surface relief grooves are generated in the dark areas. The height and shape of the final relief structure depend on the interrelation between the material components, their diffusion properties, the shrinkage of polymers, formation in the bright and dark areas, surface tension forces, and the period and intensity of the interference pattern. The decrease in the relief depth with the decreased spatial period is typical of materials with different mechanisms of the relief formation. It is connected with the general property of the interface to take a shape with a minimum area (in the equilibrium state). We observed a double increase in the surface relief depth with the introduction of 1.5 wt % Au NP to the monomer mixture. The maximum height ranging from 150 up to 400 nm depending on the grating period (Table 1) was observed. This is an additional confirmation of the NP influence on the structure, density, and consequently, contraction of the polymer network.

5. Conclusions

We present a new metal−organic nanocomposite comprising two acrylate monomers of different functionality and Au NP (1−2 wt %) suitable for the formation of the periodic structures by holographic photopolymerization. The Au NP of 1.7 and 2.7 nm core diameters were coated with an ester-terminated alkanethiol to ensure a dispersibility in the acrylic monomers and sufficient stability of the nanocomposites. The formation of the volume gratings of the period ranging from

(11) Bhargava, R. N. *J. Lumin.* **1996**, *70*, 85.

(12) (a) Smirnova, T. N.; Sakhno, O. V.; Tikhonov, E. A.; Smirnov, V. V. *Opt. Spectrosc.* **1994**, *76*, 805. (b) Croutxe-Barghorn, C.; Calixto, S.; Lougnot, D. J. *Proc. SPIE* **1997**, *2998*, 222. (c) Sakhno, O. V.; Smirnova, T. N. *Optik* **2002**, *113*, 1. (d) Sánchez, C.; de Gans, B-J.; Kozodaev, D.; Alexeev, A.; Escuti, M. J.; van Heesch, C.; Bel, T.; Schubert, U. S.; Bastiaansen, C. W. M.; Broer, D. J. *Adv. Mater.* **2005**, *17*, 2567. (e) Zhou, J.; Sun, C.; Xiong, B.; Wang, J.; Luo, Y. *Appl. Phys. Lett.* **2004**, *84*, 3019. (f) Goldenberg, L.; Sakhno, O.; Stumpe, J. *Opt. Mater.* **2005**, *27*, 1379.

(13) (a) Karpov, H. M.; Obukhovsky, V. V.; Smirnova, T. N. *Semicond. Phys. Quantum Electron. Optoelectron.* **1999**, *2*, 67. (b) Leewis, C. M.; de Jong, A. M.; van IJzendoorn, L. J.; Broer, D. J. *J. Appl. Phys.* **2004**, *95*, 4125.

0.5 up to 4.5 μm with diffraction efficiency up to 55% was achieved (in the case of PH33 Au NP). Even a small Au NP concentration was sufficient to provide a growth of n_1 from 0.0028 (for the monomer mixture) to a maximum of 0.0075 (for 1.5% NP loading). A proposed model of the grating morphology and the comparison between the calculated and experimental data show that such a high n_1 is predominantly due to the redistribution of the monomers between the grating planes rather than the periodical segregation of the NP. Therefore, Au NP are not a completely inert additive with different refractive index, which takes part only in the mass transport during holographic exposure. Based on in situ IR spectroscopy of the photopolymerization, a drastic decrease of the polymerization rate with increasing NP loading has been observed. This, probably, promotes the monomer spatial segregation and increases the refractive index modulation of the grating. This could be considered as a new mechanism of holographic grating amplification in photopolymerizable two-monomer nanocomposites. The simultaneous formation of the surface relief along with the refractive index and absorbance modulation has been revealed by AFM. The introduction of 1.5% of the Au NP leads to a double increase in the surface relief modulation that also confirms the influence of the NP on the polymer structure and, consequently, the shrinkage of the matrix in the regions of the grating corresponding to maxima and minima of the interference pattern.

The preliminary investigations have shown that the polymer−Au NP gratings exhibit significant nonlinear optical response. The relative change of the grating diffraction efficiency by more than 25% was observed in the intensity range of 0.5−2 mW/cm^2 (pulse duration is ca. 30 ps, λ_{test} = 530 nm). These effects will be reported in a separate publication.

Acknowledgment. The work was supported by the INNOWATT Project (Federal Ministry of Economics and Technology, Germany), Federal Ministry of Education and Research, Germany (International Office), and the grant of the National Academy of Science of the Ukraine (10/07-H-25c). We thank Dr. Th. Fischer (Fraunhofer IAP) for measurements with a microscope spectrometer and Dr. M. Stark (University of York) for TEM measurements.

CM8005315